Individual Domain Wall Resistance in Submicron Ferromagnetic Structures

R. Danneau,[1] P. Warin,[1] J. P. Attané,[2] I. Petej,[3] C. Beigné,[2] C. Fermon[1] O. Klein,[1]
A. Marty,[2] F. Ott,[1] Y. Samson,[2] and M. Viret[1,*]

[1]*Service de Physique de l'Etat Condensé, CEA Orme des Merisiers, F-91191 Gif-Sur-Yvette, France*
[2]*Service de Physique des Matériaux et Microstructures, CEA Grenoble, F-38054 Grenoble, France*
[3]*Clarendon Laboratory, Parks Road, Oxford, England*
(Received 27 July 2001; published 28 March 2002)

The resistance generated by *individual domain walls* is measured in a FePd nanostructure. Combining transport and magnetic imaging measurements, the intrinsic domain wall resistance is quantified. It is found positive and of a magnitude consistent with that predicted by models based on spin scattering effects within the walls. This magnetoresistance at a nanometer scale allows a direct counting of the number of walls inside the nanostructure. The effect is then used to measure changes in the magnetic configuration of submicron stripes under application of a magnetic field.

DOI: 10.1103/PhysRevLett.88.157201 PACS numbers: 75.60.Ch, 75.50.Cc, 75.60.Jk

Domain wall resistance (DWR) is a popular research topic owing to the conflicting experimental results and the theoretical difficulties encountered to explain the effect (see, for example, the review of Kent *et al.* [1]). For a long time, domain walls were considered to have no appreciable effect on the resistance of 3d ferromagnets [2]. More recently, the progress in thin film synthesis and nanolithography has allowed a more precise measure of DWR effects which have been found either positive [3–5] or negative [6]. Both findings have found theoretical justifications: Tatara and Fukuyama [7] showed that domain walls suppress weak localization, thereby removing a source of resistivity, and van Gorkom *et al.* [8] described band bending effects which could justify either negative or positive magnetoresistance (MR). Viret *et al.* [3] and Levy and Zhang [9] based their models on the giant magnetoresistance mechanism and demonstrated that spin mistracking during traversal of the rotating magnetization inside a domain wall allows diffusion events between states of opposite spins, thereby increasing the resistivity. This description has recently found strong experimental support through quantitative measurements of the domain wall resistivity anisotropy [4]. The resistivity changes associated with domain walls have also been measured in some magnetic oxides (e.g., $SrRuO_3$ [10]). However, due to the unusual transport properties of these bad metals, domain wall resistance models are no longer applicable and the domain wall contribution to the resistivity in such systems indicates the presence of other physical phenomena. Even for 3d elements, the experimental picture is still unclear since numerous papers report either negative or positive resistive contributions in unsaturated states attributed to domain walls. In this Letter, we clearly quantify the intrinsic contribution to the resistivity of individual domain walls in a nanostructure with an appropriate state of magnetization. We then demonstrate the use the DWR to probe the magnetization reversal in submicron ferromagnetic objects.

Physically, several magnetization dependent scattering processes influence electrical transport. These can be summarized in a general formula expressing the components of the electric field generated by a current density flowing through a homogeneous ferromagnet (providing Matthiessen's rule is valid):

$$\vec{E} = \rho(B)\vec{j} + \rho_{\mathrm{AMR}}(\vec{\alpha}\cdot\vec{j})\vec{\alpha} + \rho_{\mathrm{O}}\vec{B}\times\vec{j} + \rho_{\mathrm{EHE}}\vec{M}\times\vec{j} + \rho(B)\vec{dj} + \rho_{\mathrm{wall}}\vec{j}, \quad (1)$$

with $\vec{M}$ the magnetization, $\vec{\alpha}$ the unitary vector along its direction, and $\vec{B}$ the internal magnetic induction vector. The first term represents the usual longitudinal resistance contribution which varies like B^2 at low temperature (Lorentz contribution) and decreases almost linearly with B at higher temperatures (magnon damping [11]). The second term is the anisotropic magnetoresistance (AMR) which is along the magnetization direction. Its projection perpendicular to the current lines is called the planar Hall effect. The third and fourth terms are the standard Hall effects composed of the ordinary effect proportional to B and the extraordinary Hall effect (EHE) proportional to M. The fifth term, $\vec{dj}$, represents a possible deviation of the current lines while crossing different domains, such as that induced by the Hall effect [12]. The last contribution is related to the resistance due to spin scattering in domain walls.

Generally, because of the low density of domain walls (DWs), electrical transport in homogeneous ferromagnets is dominated by the AMR and the Lorentz contribution inside the domains themselves. The main experimental difficulty when one wants to measure the DW contribution is to get rid of these domain effects. In the literature, several techniques have been applied including adding resistive contributions of the same film with current lines at 0° and 90° [3] (which cancels AMR) or subtracting high field contributions (using Kholer's rule) [6]. The relevant quantity regarding magnetoresistance is the internal magnetic induction, B, which depends on the applied

field and the local demagnetizing field. The latter is the sum of contributions from all the spins which depends on sample shape and magnetic configuration. The internal field can change appreciably between saturated and multidomain states. One can argue that the local change in the internal field associated with the multidomain configuration has never properly been accounted for. The associated resistive effect can have positive or negative contributions depending on the quality of the material and the measurement temperature (normal Lorentz effect vs reduction in the magnon scattering contribution). Only in a local measurement can domain MR and DW resistance be properly separated, which is one of the aims of this Letter.

Epitaxial films such as FePd [4,5] or FePt [1,13] are ideal systems for DW resistance measurements because their perpendicular magnetic anisotropy minimizes the domain MR. The magnetization inside the domains is always perpendicular to the current, which keeps the AMR constant. Moreover, demagnetizing fields only change appreciably on a length of about twice the domain wall width, which leaves the magnetic induction constant in most of the domain volume. Then, the wiggling of the current lines induced by the Hall effect is often small at low temperature. We will check *a posteriori* that this contribution is negligible in our sample (it scales with the square of the Hall tangent which is small). We used 40-nm-thick FePd films grown by molecular beam epitaxy directly onto MgO(001) substrates with a strong perpendicular magnetic anisotropy ($K_u \approx 1.5 \times 10^6$ J/m^3). The as grown magnetic configuration of the films consists of 60-nm-wide parallel magnetic stripes separated by 8-nm-thick walls [4]. A nanostructure was made by ion milling the FePd film through a Ti mask defined by electron beam lithography and lift-off. A 400-nm-wide line was defined in a geometry with a 90° angle (like that in [10]) allowing us to measure transport in two perpendicular directions (see Fig. 1). Two 150-nm-wide contacts were left on either side of each segment, with a separation of 600 nm. On each line, the four contacts give access to both the longitudinal and transverse components of the electric field. On the magnetic force microscope (MFM) image (Fig. 1), the contrast corresponds to a reversal of the perpendicular stray field, indicating a change in the magnetic surface charges. The dark and clear ribbons correspond to up and down magnetic domains separated by domain walls which cannot be resolved by the instrument. In Fig. 1, the current flows perpendicular to the walls (CPW) on the right side of the structure and parallel to the walls (CIW) on the left side. In the initial magnetic configuration, there are six domain walls between the CPW contacts, four within the contacts, and six in the CIW segment.

The sample of Fig. 1 is placed between the poles of a 2 T electromagnet which applies a homogeneous static field perpendicular to the film in a direction that favors the white domains. The resistive and Hall voltages are measured between the different pairs of contacts at 17 K with a DC current of ±0.2 mA. The upper curve in Fig. 2 shows

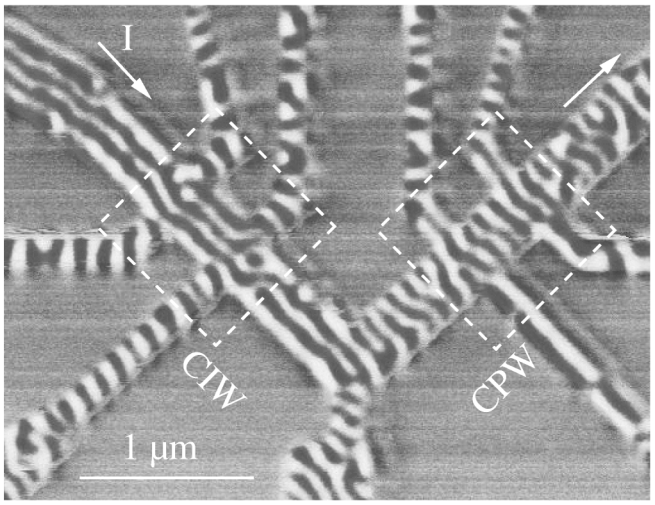

FIG. 1. Virgin magnetic configuration observed by MFM inside the FePd stripe. The dark and clear ribbons correspond to up and down magnetic domains. The current flows through the two segments of the elbow (arrows), and the resistance of each configuration, CPW and CIW, is measured between four lateral contacts.

the resistance between the two longitudinal contacts *e* and *h* as a function of magnetic field. Clear resistive jumps are observed as the field increases which are ascribed to the disappearance of domain walls. For the sake of clarity, the whole resistivity variation in Fig. 2a has been divided in eight equal parts by horizontal dashed lines. This underlines nicely the quantification of the jumps as being

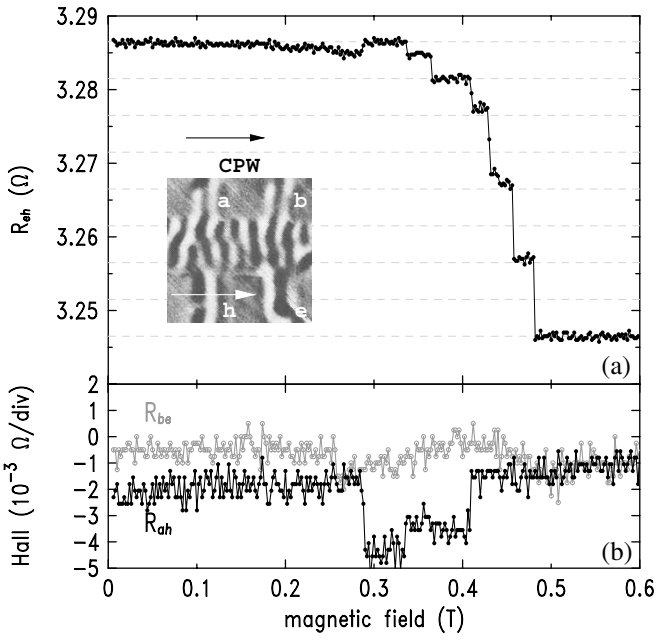

FIG. 2. Variation of resistance and Hall effect during the first magnetization sweep for the CPW configuration shown in the MFM picture. The excess resistance from the saturation value is due to domain walls. The steps are indicative of individual domain wall disappearance during the reversal process. The Hall resistance varies only during the low field single jumps, indicating that the magnetization saturates first in the contacts.

either equal to one (low field) or two (high field) elementary steps. In order to gain more insight into the interpretation of these abrupt changes, one has to turn to the Hall voltage displayed in Fig. 2b which probes the magnetization inside the contact area. There is no variation of the Hall resistivity associated with the double jumps, indicating that the corresponding magnetic reorganization occurs in the portion of the line located between the contacts. These double jumps can be ascribed to the collapse of a domain (a dark ribbon), a process through which two domain walls simultaneously disappear. As additional evidence, the number of double jumps (three) is consistent with the number of black ribbons imaged at zero field between the contacts. Conversely, variations in the Hall effect provide evidence that single jumps are due to changes in the crosses defined by the stripe and the voltage contacts. The Hall voltage (EHE) being the sum of only a few opposite domain contributions, its value largely fluctuates at low field following small changes in the micromagnetic configurations of the contacts. In the longitudinal resistance, the two corresponding single jumps are attributed to the disappearance of the two minority domains within the cross. Indeed, the voltage drop induced by one domain wall positioned within the contact is weighed by a factor close to $1/2$ depending on the exact position in the pad. A sensitivity function can be calculated which goes from zero outside the measured area (voltage not sensitive to a resistance change) to one at the other end of the cross towards the second voltage contact (resistance change completely measured) with a near plateau of $1/2$ at the center. Hence, the disappearance of two walls inside the contact appears as a single jump. The discrete elemental resistance jump corresponds to 5 mΩ giving an interface conductance of $1.2 \times 10^{16}\ \Omega^{-1}\,\mathrm{m}^{-2}$ (i.e., a magnetoresistance over 10% within the 8-nm-wide wall), in excellent agreement with the one measured in continuous films [4]. During the field sweep the magnetic configuration changes (minority domains shrink, majority domains grow [14]) inducing small variations of the internal magnetic induction. Importantly, the resistive steps are of the same amplitude for all the jumps and the resistance between the jumps remains constant (the plateaus are flat). Hence, any domain contribution to the resistance is small compared to the intrinsic wall resistance responsible for the discrete jumps. This is understandable in this system since the internal field only changes appreciably in a region of 15 nm centered on the walls, and the Hall tangent (responsible for the current wiggling) at this temperature is tiny (about 3×10^{-3}). Thus, the measurement validates the sign and amplitude of the DW resistance.

The above measurements also allow us to monitor changes in the magnetic configuration of the nanostructure during field sweeps. The observed successive collapse of minority domains can be compared with MFM observations in continuous FePd layers, where one can distinguish three processes for magnetization changes [14]. One is that the domains magnetized along the external field continuously widen in increasing field while the opposite ones shrink. This process does not change the domain wall density. Then opposite domains can roll back from their extremities, hence diminishing the minority domain size. A third possibility is that the walls straighten. These last two processes induce a decrease of the domain wall density. In our sample, wall straightening has a negligible contribution since the magnetic configuration in the virgin state is already aligned. Our resistive measurements indicate that the width contraction of the minority domains is the dominant magnetization growth mechanism below 0.2 T. Then, the collapse of minority domains takes place first in the contacts and then in the narrow stripe. This indicates that the nanostructure enhances the saturation field most probably because of pinning at the sample edges. As one opposite domain disappears, the subsequent modification of the local demagnetizing field pushes the collapse of the neighboring one towards higher field. This helps to spread the reversal fields at which walls disappear and induces the successive occurrence of the collapse events.

We now turn our attention to the other branch of the sample, where the walls are parallel to the stripe. Figure 3 shows the measured resistance variation during the first magnetization curve. Here, since six domain walls are counted at zero field between the stripe's edges, we divided the total resistance variation in six equal steps. These agree well with the measured resistance plateaus. The size of the individual steps (3 mΩ) are noticeably smaller than the ones measured in the CPW configuration

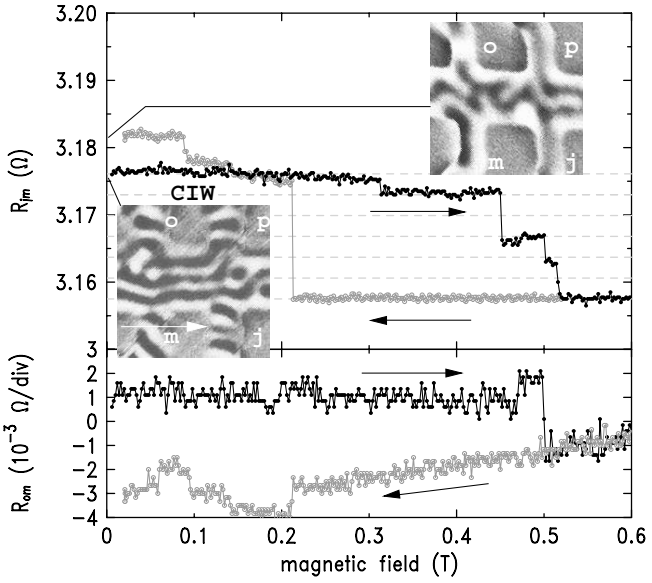

FIG. 3. The black curves are measurements of the resistance and Hall effect in the CIW configuration during the first magnetization process. The left inset is a MFM picture of the initial magnetic configuration. The grey curve shows the same quantities as the field is swept back to zero. The abrupt jump at 0.213 T corresponds to the nucleation of domains. The right inset is a MFM image of the nucleated domain configuration in the remanent state.

(in spite of the longer walls involved), leading to a wall magnetoresistance of 3%, again in good agreement with the CIW effect observed in a continuous layer [4]. There are also double and single jumps. We again attribute the double jumps to the full collapse of black ribbons which is associated with the disappearance of two walls. The single jumps correspond to the disappearance of peripheral domain walls expelled one by one through the lateral edges of the structure. Looking back more carefully at the MFM image, we infer that the latter displacement affects more likely the upper dark ribbon located between contacts o and p. According to the even number of walls observed on the MFM image, their disappearance should lead to an even number of single jumps, as observed in the resistivity. The two double jumps are associated with the collapse of the two interior black ribbons. Here again one can notice the negligible amplitude of the resistive contribution from the domains.

We now consider the events occurring when decreasing the field from saturation. A large resistance step at $B = 0.213$ T is measured in both segments of the stripe, indicating the reappearance of domain walls. This nucleation of reversed domains occurs well below the saturation field and is also visible in the Hall effect which changes abruptly at the same field. Hence, reversed domains appear everywhere in the structure at the same field which suggests that the reversal process is dominated by domain wall propagation from a few nucleation centers. Once back to zero field and room temperature, the magnetic configuration is visualized by MFM (see the upper right inset of Fig. 3). On the image all the reversed regions within the line are connected to the same domain which extends far in the current pads. This is consistent with the conclusions drawn from resistance measurements. It is also in agreement with the scarce nucleation events observed in the continuous layer [14]. Because the nucleation process in our film is not controlled, the winding geometry of the walls leads to a mixture of both CIW and CPW contributions to the resistance. Branching events are also visible on the MFM image which might be responsible for the subsequent smaller steps in the resistivity data. A better reversibility of the magnetization process could be achieved by the introduction of well-controlled defects or constrictions in the lines acting as nucleation centers.

In conclusion, this paper demonstrates that there exists a measurable excess resistance attached to the domain walls in 3d ferromagnetic nanostructures. The amplitude of the effect in FePd when the current flows perpendicular to the wall reaches 10% (within the wall). Coupled resistance and Hall measurement represent an excellent tool to monitor magnetization reversal in mesoscopic elements, especially as regard sensitivity and speed. Here, we were able to measure the (dis)appearance of a single domain wall which, in our sample, corresponds to the canting of about 5×10^6 spins. In the future, these measurements could be extended to probe the dynamics of magnetization reversal beyond the nanosecond time scale. Other resistive measurements (using giant and tunneling magnetoresistance structures) lead to the variation of M and have already been used to follow magnetization reversal in nanostructures. DW resistance is different in that it does not directly probe changes in magnetization but gives domain wall density information (i.e., an average domain size). This effect is interesting since the total resistance remains constant while M varies reversibly and only shows up as discrete calibrated jumps when domains disappear (and M becomes irreversible). Conceptually, in our geometry, this corresponds to a multilevel measurement, as single resistivity data allow us to count directly the number of domain walls within the line. Further progress may be to extend these measurements to constricted geometries, where the DW width scales with the constriction size. Since the DW resistivity is predicted to scale inversely with the square of the DW width [3,9], larger resistive effects should be generated.

We thank the European Union for financial support through two contracts: DYNASPIN (TMR Ref. FMR-X-CT97-0124) and MAGNOISE (IST-1999-10486).

*Corresponding author.
Electronic address: mviret@cea.fr

[1] A. D. Kent, J. Yu, and S. S. P. Parkin, J. Phys. Condens. Matter **13**, R461 (2001).
[2] G. G. Cabrera and L. M. Falicov, Phys. Status Solidi **61**, 539 (1974).
[3] M. Viret, D. Vignoles, D. Cole, J. M. D. Coey, W. Allen, and J. F. Gregg, Phys. Rev. B **53**, 8464 (1996).
[4] M. Viret, Y. Samson, P. Warin, A. Marty, F. Ott, E. Sondergard, O. Klein, and C. Fermon, Phys. Rev. Lett. **85**, 3962 (2000).
[5] D. Ravelosona, A. Cebollada, F. Briones, C. Diaz-Paniaga, F. Hidalgo, and F. Batallan, Phys. Rev. B **59**, 4322 (1999).
[6] U. Ruediger, J. Yu, S. Zhang, A. D. Kent, and S. S. P. Parkin, Phys. Rev. Lett. **80**, 5639 (1998); S. G. Kim, Y. Otani, K. Fukamichi, S. Yuasa, M. Nyvlt, and T. Katayama, IEEE Trans. Magn. **35**, 2862 (1999).
[7] G. Tatara and H. Fukuyama, Phys. Rev. Lett. **78**, 3773 (1997).
[8] R. P. van Gorkom, A. Brataas, and G. E. W. Bauer, Phys. Rev. Lett. **83**, 4401 (1999).
[9] P. M. Levy and S. Zhang, Phys. Rev. Lett. **79**, 5110 (1997).
[10] L. Klein, Y. Kats, A. F. Marshall, J. W. Reiner, T. H. Geballe, M. R. Beasley, and A. Kapitulnik, Phys. Rev. Lett. **84**, 6090 (2000).
[11] B. Raquet, M. Viret, P. Warin, E. Sondergard, and R. Mamy, Physica (Amsterdam) **294B**, 102 (2001).
[12] L. Berger, J. Appl. Phys. **49**, 2156 (1978).
[13] J. Yu, U. Ruediger, A. D. Kent, R. F. C. Farrow, R. F. Marks, D. Weller, L. Folks, and S. S. P. Parkin, J. Appl. Phys. **87**, 6854 (1999).
[14] O. Klein, Y. Samson, A. Marty, S. Guillous, M. Viret, C. Fermon, and H. Alloul, J. Appl. Phys. **89**, 6781 (2001).